PHYSICAL REVIEW D **83,** 054013 (2011)

Uncertainties on exclusive diffractive Higgs boson and jet production at the LHC

A. Dechambre,[1,2] O. Kepka,[3] C. Royon,[2] and R. Staszewski[4,2]
[1]*IFPA, Dept. AGO, Université de Liège*
[2]*CEA/IRFU/Service de physique des particules, CEA/Saclay*
[3]*Center for Particle Physics, Institute of Physics, Academy of Science, Prague*
[4]*Institute of Nuclear Physics, Polish Academy of Sciences, Krakow*
(Received 7 January 2011; published 9 March 2011)

Two theoretical descriptions of exclusive diffractive jets and Higgs production at the LHC were implemented into the FPMC generator: the Khoze, Martin, Ryskin model and the Cudell, Hernández, Ivanov, Dechambre exclusive model. We then study the uncertainties. We compare their predictions to the CDF measurement and discuss the possibility of constraining the exclusive Higgs production at the LHC with early measurements of exclusive jets. We show that the present theoretical uncertainties can be reduced with such data by a factor of 5.

DOI: 10.1103/PhysRevD.83.054013 PACS numbers: 14.80.Bn, 13.85.Rm

I. INTRODUCTION

The Higgs boson is the last particle of the standard model remaining to be confirmed experimentally. Inclusive searches in decay channels such as $b\bar{b}$, W^+W^-, ZZ, $\gamma\gamma$ and associated production have been performed at the Tevatron and are being started at the LHC. However the search for the Higgs boson at low mass is complicated due to the huge background coming from QCD jet events. Especially the $b\bar{b}$ channel, dominant for $m_H = 120$ GeV, is very difficult at the Tevatron and literally impossible at the LHC. Thus other possibilities have been investigated, in particular, using the exclusive diffractive production [1,2]. In such processes both incoming hadrons, $p\bar{p}$ at the Tevatron and pp at the LHC, remain intact after the interaction and the Higgs decays in the central region. The process involves the exchange of a color singlet and large rapidity gaps remain between the Higgs and the outgoing hadrons. At the Tevatron it is not possible to produce exclusively the Higgs boson due to the tiny cross section. However other particles, or systems of particles, can be produced, i.e. a pair of jets (a dijet), χ_c or $\gamma\gamma$, as long as they have 0^{++} quantum numbers [1]. Note that production of exclusive χ_c with quantum numbers 1^{++} or 2^{++} [3,4] and dijet in 2^{++} state [5] can also be noticeable but the dominance of the zero state still holds.

Since the incoming hadrons remain intact, lose a part of their energy and are scattered at very small angles, it is experimentally possible to measure all final state particles, including the scattered protons. This can be done using detectors inserted close to the beam pipe at a large distance from the interaction point. Besides, at the Tevatron and for low luminosity at the LHC, it is also possible to use the rapidity gap method to select such events. A big advantage of the exclusive production of the Higgs boson is a very accurate mass determination from the measurement of the scattered proton energy loss [6,7]. In addition, if the Higgs is observed in this mode at the LHC it ensures it is a 0^{++} particle.

The plan of this paper is as follows. In Sec. II we give an introduction to the theoretical description of exclusive production and introduce two models: the Khoze, Martin, Ryskin (KMR) and the Cudell, Hernández, Ivanov, Dechambre exclusive (CHIDe) model, and also discuss the sources of their uncertainties. In Sec. III the Forward Physics Monte Carlo (FPMC) program is presented and the implementation of both models is discussed. Section IV focuses on the CDF measurement of exclusive jets production and shows that both models give similar, reasonable descriptions of the data. In Sec. V we analyze the uncertainties using the CHIDe model as an example. Predictions for exclusive production at the LHC are given in Sec. VI, where in addition we study the possibility of constraining the Higgs production at the LHC from early LHC exclusive jets measurement. Finally, conclusions are given in Sec. VII.

II. THEORETICAL DESCRIPTION

The exclusive production can be modeled in the QCD framework where the process was described as a two-gluon exchange between quarks—one gluon involved in the production and the other one screening the color. Such calculation requires an analytic evaluation of a set of Feynman diagrams that describe the production of a color singlet and keep the color of initial particles, *e.g.* Fig. 1(a). The calculation is well known and under theoretical control [1,8–11]. It can be performed using cutting rules or direct integration within the kinematic regime where the momentum lost by the initial particles is small.

However this simple model is not enough and, to make a description more realistic, soft and higher order corrections need to be added, see [1,12]:

The impact factor [13–15] regulates the infrared divergence and embeds quarks inside the proton as represented in Fig. 1(b). The impact factor is based on a skewed unintegrated gluon density but its exact form depends on the model considered.

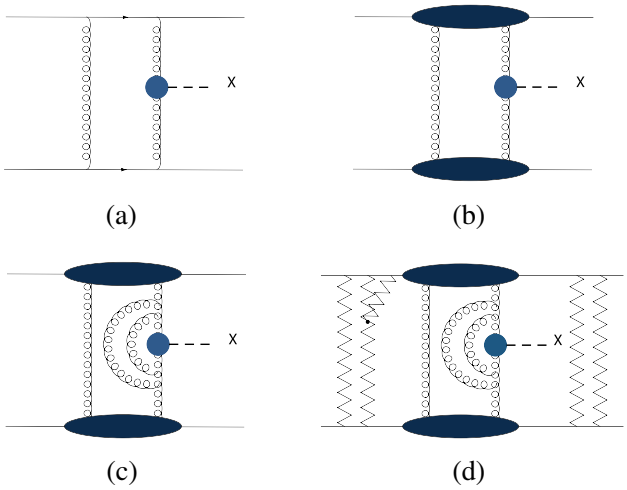

FIG. 1 (color online). Schematic representation of the standard scheme of the exclusive cross section calculation with its various steps. (a) Parton level calculation, (b) impact factor, (c) Sudakov form factor and (d) rescattering corrections.

The Sudakov form factor [16–18] is one of the most important ingredients of the calculation. It corresponds to virtual vertex correction [see Fig. 1(c)] and depends on two scales. The hard scale is linked to the hard subprocess ($gg \to X$). The soft scale is related to the transverse momentum of the active gluons—the scale from which a virtual parton can be emitted. The Sudakov form factor suppresses the cross section by a factor of the order of 100 to 1000.

Finally, additional pomeron exchanges between the initial and final state protons can occur [19], as schematically shown in Fig. 1(d). This can lead to the production of additional particles that might fill the gap created at the parton level. It is taken into account by introducing the rapidity gap survival probability, which is a probability of not having any additional soft interactions.

Each piece of the calculation can be investigated separately and its uncertainties can be estimated. The important point is that some of the corrections are identical in all exclusive processes so that they can be studied in one particular process and used to predict the cross section of any process.

A. The KMR Model

The most quoted and first complete calculation is done in the Khoze, Martin and Ryskin (KMR) model from the Durham group. One can find here the main lines, referring the reader to [1,16] for a review.

The cross section (σ) of the process represented schematically in Fig. 2(a), is assumed to factorize between the effective luminosity $\mathcal{L}$ and the hard subprocess $\hat{\sigma}$:

$$\sigma = \mathcal{L} \times \hat{\sigma}(gg \to X), \tag{1}$$

where X is the centrally produced system. In particular,

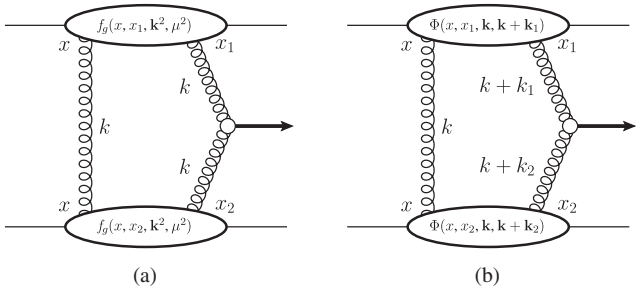

FIG. 2. Schematic representation of the exclusive diffractive production amplitude in the: (a) KMR model, (b) CHIDe model.

$$\frac{\partial \sigma}{\partial s \partial y \partial \mathbf{P}^2 \partial \mathbf{Q}^2} = S^2 e^{-B(\mathbf{P}^2+\mathbf{Q}^2)} \frac{\partial \mathcal{L}}{\partial s \partial y} d\hat{\sigma}(gg \to H). \tag{2}$$

The different variables are, the energy in the center-of-mass frame s, the rapidity of the centrally produced system y and the transverse momenta of the final protons $\mathbf{P}^2$ and $\mathbf{Q}^2$. One can also recognize in turn, the gap survival probability S^2 and the t slope of the cross section with $B = 4$ GeV^2 (taken from the fit to the soft hadronic data [1]), introduced assuming that the dependence of the hard cross section on the final proton transverse momentum is small. The subprocess cross section for Higgs production, $\hat{\sigma}(gg \to H)$, includes an additional factor K fixed to 1.5, which takes into account next-to-leading-order corrections. The effective luminosity is given by

$$\frac{\partial \mathcal{L}}{\partial s \partial y} = \left(\frac{\pi}{(N_c^2 - 1)} \int \frac{d\mathbf{k}^2}{\mathbf{k}^4} f_g(x, x_1, \mathbf{k}^2, \mu^2) f_g(x, x_2, \mathbf{k}^2, \mu^2) \right)^2, \tag{3}$$

μ is the hard scale and the variables are defined in Fig. 2(a). The function f_g stands for the unintegrated skewed gluon density related to the conventional integrated gluon distribution function and taken here in their simplified form [13]:

$$f_g(x, x_1 \gg x, \mathbf{k}^2, \mu^2) = R_g \frac{\partial}{\partial \log \mathbf{k}^2} [\sqrt{T(\mathbf{k}, \mu)} x g(x, \mathbf{k}^2)]. \tag{4}$$

The factor R_g account for the skewness (the fact that $x_1 \gg x$; $g(x, \mathbf{k}^2)$ describes the forward gluon density only when $x = x_1$) and is found to be about 1.2 at the LHC energy of 14 TeV. One can note that the Sudakov form factor $T(\mathbf{k}, \mu)$

$$T(\mathbf{k}, \mu) = \exp\left[- \int_{l^2}^{\mu^2} \frac{d\mathbf{q}^2}{\mathbf{q}^2} \frac{\alpha_s(\mathbf{q}^2)}{2\pi} \times \int_0^{1-\Delta} \left(z P_{gg}(z) + \sum_q P_{qg}(z) \right) dz \right], \tag{5}$$

with $\mathbf{q}$ and z the transverse and longitudinal components of the additional emission, is here included in the differentiation. P_{gg} and P_{qg} are the quark and gluon splitting

functions. In the KMR model, the presence of the Sudakov form factor makes the integration infrared stable and it is assumed to provide applicability of perturbative QCD. According to a calculation at single-log accuracy of the Durham group [1]:

$$\Delta = \frac{|\mathbf{q}|}{|\mathbf{q}| + \mu}, \qquad \mu = 0.62 m_X, \tag{6}$$

where m_X is the mass of the centrally produced system. These results were recently reevaluated in [17] giving new values for Higgs production:

$$\Delta = \frac{|\mathbf{q}|}{\mu}, \qquad \mu = m_H. \tag{7}$$

This correction leads to approximately a factor 2 suppression in the cross section.

The KMR model has been developed for years and is one of the most complete since it includes different types of exclusive diffractive production, i.e. from Higgs, dijet, $\gamma\gamma$, di-quark, $\chi_c, \ldots$ to supersymmetric particles, and shows results in agreement with the available data [20].

B. The CHIDe Model

In this paper, we also consider the Cudell, Hernández, Ivanov, Dechambre exclusive (CHIDe) model [5] for jets and SM Higgs boson production. The structure of this model is similar to the one of the KMR model but differs in the implementation and details of the different ingredients. Namely, the same kind of exclusive mechanism is used for exclusive production, but, in particular, nonperturbative ingredients are treated differently. The CHIDe model separates the Sudakov form factor from the skewed gluon density definition. We detail the differences between both models in the following. In the CHIDe model the cross section for the exclusive process shown in Fig. 2(b) is given by

$$\sigma \simeq S^2 \Bigg[\int \frac{d^2\mathbf{k} d^2\mathbf{k}_1 d^2\mathbf{k}_2}{\mathbf{k}^2 (\mathbf{k}+\mathbf{k}_1)^2 (\mathbf{k}+\mathbf{k}_2)^2} \times \Phi(x, x_1, \mathbf{k}, \mathbf{k}+\mathbf{k}_1) \Phi(x, x_2, \mathbf{k}, \mathbf{k}+\mathbf{k}_2) \times \sqrt{T(\ell_1, \mu)}\, \mathcal{M}(gg \to X) \sqrt{T(\ell_2, \mu)} \Bigg]^2, \tag{8}$$

where Φ is the impact factor, $T(\ell_i, \mu)$ is the Sudakov form factor, $\mathcal{M}(gg \to X)$ is the hard subprocess amplitude, and the transverse momenta $\mathbf{k}$, $\mathbf{k}_1$, $\mathbf{k}_2$ are defined as in Fig. 2(b). In the whole calculation of the exclusive cross section, the exact transverse kinematics is kept in all ingredients and the possibility of final state, in particular, dijet system, with quantum numbers 2^{++} is taken into account. Contrary to the KMR model the color neutrality of the proton is implemented independently of the Sudakov suppression in the impact factor. It includes the skewed unintegrated gluon density and this phenomenological model of the proton includes soft physics based on both the data (elastic cross section, proton structure functions) and theory (dipole picture, light-cone wave functions). It takes into account the proton wave function as the impact factor goes to zero if one of the transverse momentum of the t-channel gluons goes to zero and the nonzero transverse momentum transfer is introduced via a universal exponential factor. The unintegrated gluon density is built on the sum of two terms that take care, respectively, of the hard and soft behavior of the proton structure function. The hard component is based on direct differentiation of the well-known gluon density (GRV [21], MRS [22] and CTEQ [23]). The soft component models soft color singlet exchanges in the nonperturbative regime in the spirit of the dipole picture. This gives space for a contribution of the nonperturbative regime of QCD. It was made in a phenomenological way and therefore is not unique. Actually, four different fits are provided, all giving similar χ^2 when adjusted to the F_2 data [24,25]. The main difference between the fits is the parametrization of the soft region—in particular, the transition scale from the soft to the hard regime. They represent the present uncertainty on the unintegrated gluon distributions.

The Sudakov form factor is identical to Eq. (5). The upper limit is taken at the Higgs mass according to the recent result [17] in the Higgs case but for dijet production it is fixed to the hard-transverse momentum in the vertex. Note that in this model $\Delta = |\mathbf{q}|/\mu$ and NLO corrections (K factor) were also introduced for the Higgs production.

C. Theoretical uncertainties

The parton level computation is well understood and very precise. However the impact factor, Sudakov form factor and rapidity gap survival probability cannot be calculated perturbatively and have to be modeled or parametrized. This introduces non-negligible uncertainties that need to be discussed.

Three main sources of uncertainties can be identified concerning the prediction of the exclusive jet or Higgs boson cross section. The first one is the uncertainty on the gap survival probability. At pp or $p\bar{p}$ colliders additional soft interactions can destroy the gap in forward region or even the proton itself. While the Tevatron measurement leads to a survival probability of 0.1, the value at the LHC is still to be measured. We assume in the following a value of 0.03 at the LHC [26] and all mentioned cross sections need to be corrected once the value of the survival probability has been measured.

The two other sources of uncertainties and their effects on the exclusive cross sections, namely, the uncertainty on the unintegrated gluon distribution in the proton and the constant terms in the Sudakov form factor, will be discussed in the next paragraphs. In the CHIDe model, the gluon density in the impact factor contains a soft and a hard part. The hard part is known very well, mainly from the DIS structure function F_2 and vector meson data [15], but

the soft one comes from a phenomenological parametrization which leads to uncertainties in both the dijet and the Higgs calculation.

In the dijet exclusive cross section, the main uncertainty comes from the limits of the Sudakov integral, which have not yet been fixed by a theoretical calculation. The lower limit is related to the transverse momentum of the active gluons and the upper to the hard scale of the process. In the case of a pointlike-vertex, these values were estimated first by KMR [1] then corrected afterward by Coughlin and Forshaw [17], they are fixed independently to reproduce the dominant log contribution from the vertex correction. If the vertex is not pointlike, it exists no calculation of the Sudakov correction, the log structure is not known and the choice of the limits is not dictated by QCD except to be related to the soft and hard scale of the process. Therefore instead of Eq. (5) in the CHIDe model the following is used:

$$T(l_i, \mu) = \exp\Bigg[- \int_{l_i^2/x'}^{\mu^2/x} \frac{d\mathbf{q}^2}{\mathbf{q}^2} \frac{\alpha_s(\mathbf{q}^2)}{2\pi} \times \int_0^{1-\Delta} \Big(z P_{gg} + \sum_q P_{qg}(z) \Big) dz \Bigg], \quad (9)$$

where two additional parameters, x and x', are included. We did not want to diverge too much from the prediction of the pointlike case and choose to vary the two parameters as described in Sec. V. In the Higgs exclusive case, the log structure of the Sudakov form factor has been calculated to single-log accuracy and the complete one loop result can be taken into account by adjusting the upper limit to $\mu = m_H$, the lower limit is $\mathbf{k} + \mathbf{k}_i$ with $i = 1, 2$. However, this calculation does not take into account the importance of the constant terms that cannot be exponentiated but have important contributions when the coupling is running [5]. To evaluate this theoretical uncertainty, we include the effect of changing the constant terms by changing the lower scale. It is possible as it was shown in [27] that this change mimics the uncertainty coming from a factor 2 in the constant terms. Eventually, it gives a upper bound for the uncertainty on the Higgs exclusive calculation because no uncertainty is related to the lower scale itself [28].

We discuss these uncertainties in more detail in Sec. V, where we study the effect of varying these parameters and changing the gluon densities. We also compare the results to the existing data.

III. THE FORWARD PHYSICS MONTE CARLO

All models described above have been implemented in the Forward Physics Monte Carlo (FPMC) [29], a generator that has been designed to study forward physics, especially at the LHC. It aims to provide the user a variety of diffractive processes in one common framework using HERWIG [30] for hadronization. In particular the following processes have been implemented in FPMC: single diffraction, double pomeron exchange, central exclusive production (including the direct implementation of KMR and CHIDe models) and two-photon exchange (including anomalous couplings between gauge bosons).

The implementation of the KMR and CHIDe models in FPMC allows a direct comparison of both models using the same framework. In Fig. 3, we display the cross section of exclusive Higgs boson production at the LHC for a center-of-mass energy of 14 TeV as a function of the Higgs boson mass. In addition, we display the predictions from the KMR original calculation [31] and the results of the implementation of the KMR model in the ExHuME generator [32]. The difference in the results between the FPMC and ExHuME implementations of the KMR model is the effect of two factors. The first one is the different treatment of the gluon distribution in Eq. (3). In ExHuME the value of the gluon distribution is frozen for small $\mathbf{k}^2$ (about 1 GeV), whereas in FPMC we integrate from $\mathbf{k}^2 = 2$ GeV^2. In fact both solutions can lead to uncertainties, therefore the better way is to introduce the modeling of the soft region, which has been done in the CHIDe model. The other reason of the disagreement between FPMC and ExHuME is the different implementation of the hard subprocess. In FPMC the Higgs is produced and then its decay is performed, whereas the ExHuME implementation involves calculation of the Higgs propagator. The difference on the Higgs production cross section between the KMR and CHIDe models is clearly visible. The CHIDe model leads to a smaller cross section and shows a steeper dependence on the Higgs boson mass. A similar difference between models can be observed for the exclusive jet production at the LHC, see Fig. 4. The cross section obtained with the KMR model is higher than the CHIDe prediction and a difference in slope is also visible. However, as we will see in the following, these differences are within the uncertainties of the models.

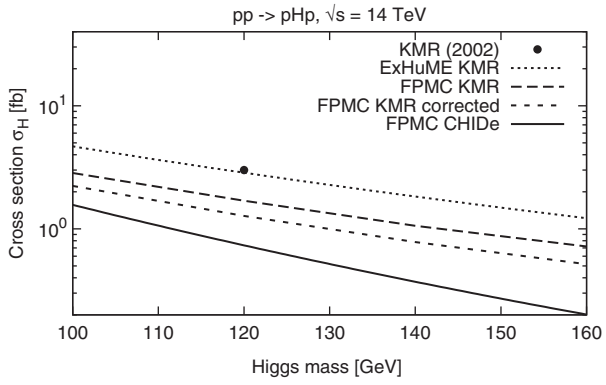

FIG. 3. Cross section for exclusive Higgs boson production at the LHC as a function of the Higgs boson mass. Predictions of CHIDe and KMR implemented in FPMC are presented. For comparison the implementations of the original KMR model [31] (black point) and ExHuME generator are given. In addition the effect of changing the upper scale from $0.62 m_H$ to m_H in Eq. (7) on the KMR model is presented (FPMC KMR corrected).

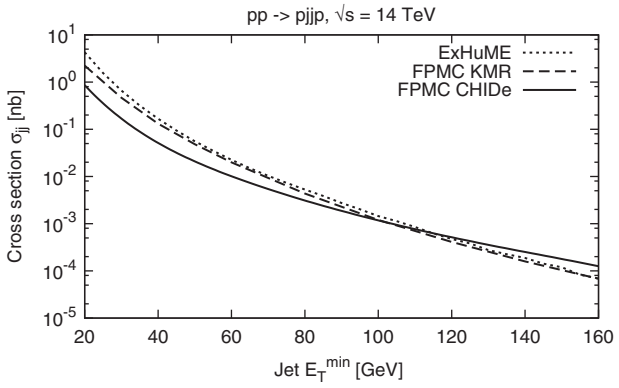

FIG. 4. Cross section for exclusive jet production at the LHC as a function of of the minimum jet E_T. Predictions of CHIDe and KMR are presented. For comparison the results of the ExHuME generator are given.

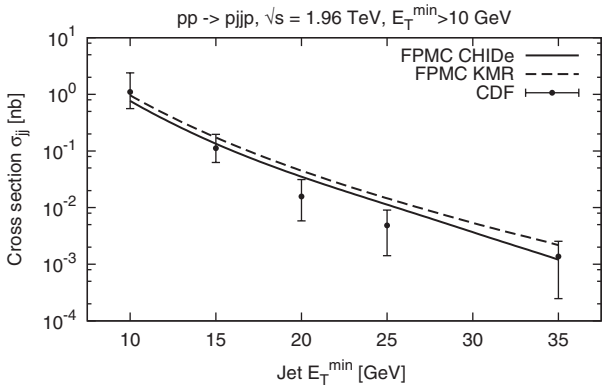

FIG. 5. Exclusive jet production cross section at the Tevatron as a function of the minimum jet E_T. The CDF measurements are compared to the CHIDe and KMR models displayed after applying the CDF jet algorithm.

In order to compare the KMR and CHIDe models with the measurements performed by the CDF Collaboration at the Tevatron the output of the FPMC generator was interfaced with a cone jet algorithm of radius 0.7 as used by the CDF Collaboration.

IV. COMPARISON TO THE CDF MEASUREMENT

To test the KMR and CHIDe models and their implementation in FPMC, the first step is to compare their predictions with the measurements performed in the CDF Collaboration at the Tevatron. The advantage of FPMC is that we can compare directly the theoretical calculations with the CDF measurement since we use, at the particle level, a 0.7 jet cone algorithm as used by the CDF Collaboration. CDF measured the so-called dijet mass fraction as a function of the jets minimum transverse energy $E_T^{\min}$ after tagging the antiproton in dedicated roman pot detectors, and requesting a rapidity gap devoid of any activity in the proton direction to ensure that only double pomeron exchange events are selected. The dijet mass fraction is defined as the ratio of the dijet mass divided by the total mass of the event computed using the calorimeter. If an exclusive event is produced, it is expected that the dijet mass fraction will be close to 1 since only two jets and nothing else are produced in the event. On the contrary, inclusive diffractive events show some energy loss due to pomeron remnants and the dijet mass fraction will be mainly distributed at values lower than 1. The dijet mass fraction distribution allowed the CDF Collaboration to separate the exclusive and inclusive diffractive contributions and to measure the exclusive diffractive dijet cross section as a function of the minimum jet E_T [33].

The predictions of the KMR and CHIDe models are compared to the CDF measurement in Fig. 5. A good agreement is found between the CDF measurement and the predictions of both CHIDe and KMR models and the difference between the models is small compared to the data uncertainties. One should notice that the data suggest slightly different dependence on $E_T^{\min}$ that the models, however it can just be a matter of statistical fluctuation.

Figure 6 displays the dijet mass (M_{jj}) distribution predicted by the KMR and CHIDe models. The difference in slope is very small, KMR leading to a slightly steeper dependence.

In addition to the jet E_T threshold dependence, the CDF Collaboration published the exclusive jets cross section as a function of the dijet mass. The dijet mass cross section is not a direct measurement but was extracted by the CDF Collaboration from the jet E_T threshold cross section data. The method is to compare the prediction of a given model (for instance KMR) with the direct measurement of the jet E_T threshold cross section. The MC predictions are then reweighted to the CDF measurement in each bin of $E_T^{\min}$ (namely 10, 15, 20, 25, and 30 GeV) to obtain the CDF exclusive dijet mass cross section ''measurement''. The CDF measurement can then be compared to the KMR or CHIDe models. It is worth noticing that this method is

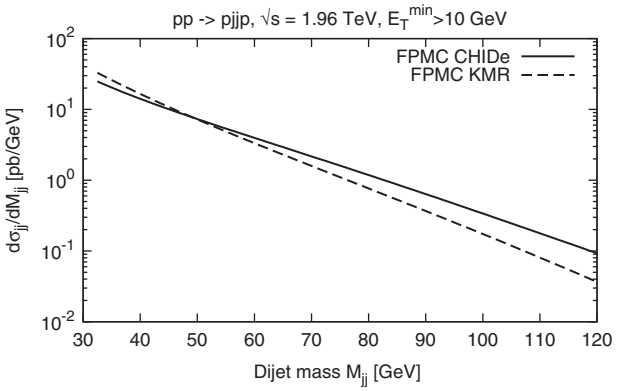

FIG. 6. Dijet mass cross section for exclusive jet production at the Tevatron for the CHIDe and KMR models.

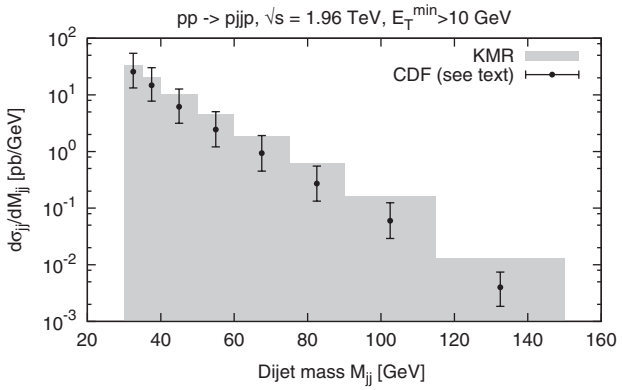

FIG. 7. Dijet mass distribution extracted from the CDF measurement of exclusive jet production compared to the KMR model.

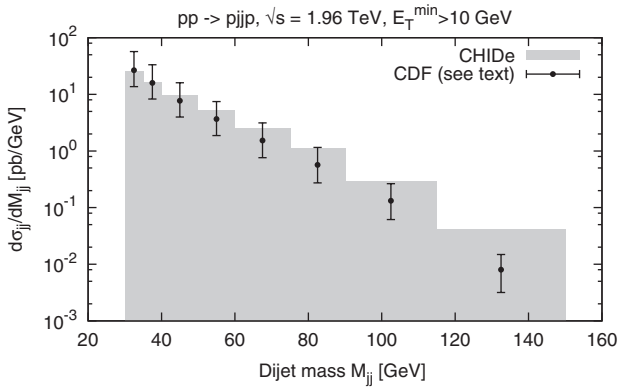

FIG. 8. Dijet mass distribution extracted from the CDF measurement of exclusive jet production compared to the CHIDe model.

clearly MC dependent since there is not a direct correspondence between the jet E_T and dijet mass dependence. This is why we had to redo this study independently for each model, namely, KMR and CHIDe.

The comparisons between the CDF ''measurements'' and the models predictions are given in Figs. 7 and 8 for the KMR and CHIDe models, respectively. We stress once more that the CDF measurements, displayed in both figures as black points, are model-dependent because of the method used to extract them, and the ''data'' points are different in both figures. We note a good agreement between the CDF extracted measurements and the KMR and CHIDe models displayed as gray histograms.

V. MODEL UNCERTAINTIES

After having compared both KMR and CHIDe predictions to the present available high-mass measurements from the Tevatron, we discuss in this section the uncertainties of the model predictions especially for exclusive Higgs boson production at the LHC. In the following we discuss the uncertainties of the CHIDe model.

To check the uncertainty due to the gluon distributions four different parameterizations of unintegrated skewed gluon densities are used to compute the exclusive jets and Higgs boson cross sections. As we mentioned in Sec. II, these four gluon densities represent the uncertainty spread due to the present knowledge on unintegrated parton distribution functions. The first step is to check if these different unintegrated gluon distributions are compatible with data. Figure 9 shows the comparison between the CDF measurement and the predictions of the CHIDe model using the four different gluon distributions described above. All gluon densities lead to a fair agreement with the data. The measurement seems to favor FIT 4, but one needs to remember that other parameters of the model, such as the cutoff used in the Sudakov form factor can modify the cross section as we will see in the following. There is an interplay between the different gluon distributions and the scales used in the model. The default gluon density used in the CHIDe model is FIT 4, which shows the highest soft contribution and predicts the highest cross section. Figures 10 and 11 show the predictions of the CHIDe model with the same four gluon densities for the exclusive dijet and exclusive Higgs at the LHC. The uncertainty on the exclusive cross sections due to the different gluon distributions is about a factor of 3.5 for jets and 2 for Higgs boson, respectively.

For Higgs boson production at the LHC the uncertainty coming from the different FITs is given by Fig. 11. Using FPMC, one has the possibility to study the uncertainty coming from the use of unintegrated gluon density in models similar to the KMR model. This is done by changing the lower cutoff in the unintegrated gluon. The bands showed in Figs. 10 and 19 correspond to a variation of this cutoff on the gluon distribution from 1.26 GeV^2 (the minimal value at which the gluon distribution MRST2002 is known) to 3 GeV^2. The difference is small but not negligible.

In addition to the uncertainty due to the unintegrated gluon distribution, we consider the additional uncertainties due to the values of integration limits in the Sudakov form

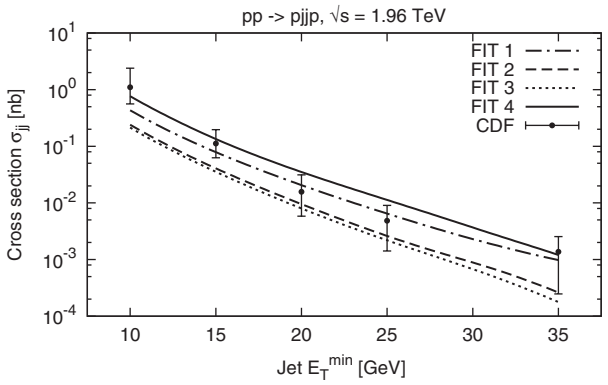

FIG. 9. Effect of changing the gluon distribution on the exclusive jet production at the Tevatron.

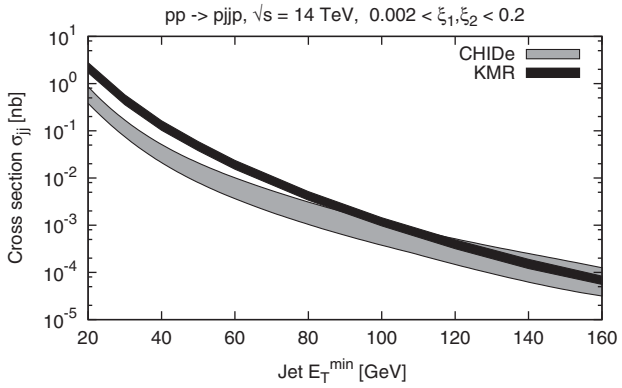

FIG. 10. Effect of changing the gluon distribution on the exclusive jet production at the LHC.

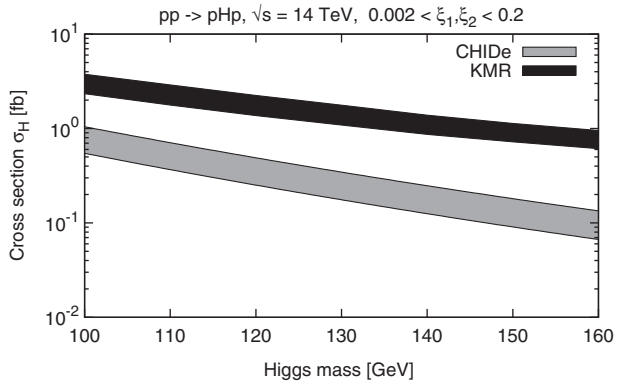

FIG. 11. Effect of changing the gluon distribution on the exclusive Higgs production at the LHC.

factor, see Eq. (9). Contrary to the KMR model, the CHIDe model does not fix the limits of integration in the Sudakov form factor in the dijet case. In the Higgs case, the upper scale is fixed to m_H and only the lower scale can be varied as explained in Sec. II C .

The lower integration limit is given by the x' parameter and the default value for FIT4 is 0.5, originally chosen [27] to describe the CDF data. Increasing the x' value increases

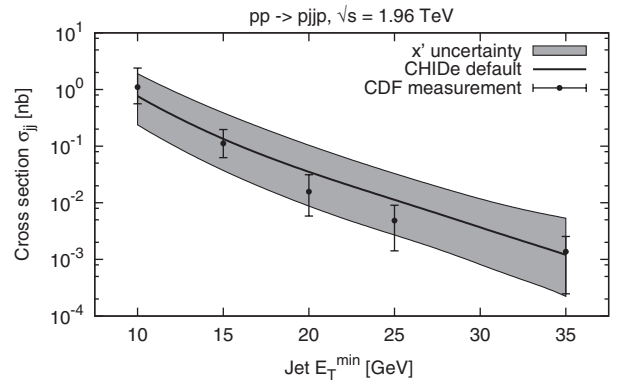

FIG. 12. Effect of varying the lower limit of the Sudakov form factor on the exclusive jets production at the Tevatron.

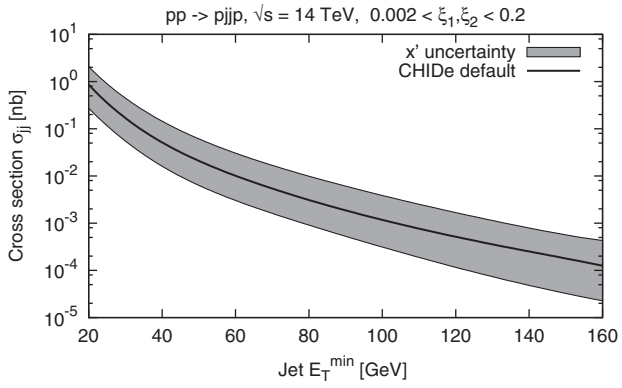

FIG. 13. Effect of varying the lower limit of the Sudakov form factor on the exclusive jets production at the LHC.

the values of the integral and reduces the cross section. Decreasing x' leads to the opposite. Varying x' by a reasonable factor of 2 up and down modifies the cross section by a large factor up to 5 for all considered processes, namely, jet production at the Tevatron (see Fig. 12), jet production at the LHC (see Fig. 13) and Higgs boson production at the LHC (see Fig. 14).

The upper limit of the integration is specified by the parameter x. As already mentioned in Sec. II, the value of the upper limit for the Higgs boson production has been fixed by the calculation to 1.0 ($\mu = m_H$). Although it still contributes to the total uncertainty for the jet production cross section, its effect is much smaller for lower limit (see Figs. 15 and 16 for the jet cross section at the Tevatron and at the LHC, respectively). The default value of the x parameter is 0.5, which we vary again by a factor 2. Decreasing its value leads to an increase of the jet cross section. The effect is indeed visible at Tevatron energies (Fig. 15) while it is negligible at the LHC for $E_T^{\min}$ above 50 GeV (Fig. 16). It should be noted that this is quite different from changing the x' parameter.

From this analysis it follows that the uncertainty related to the exclusive diffractive production is dominated by the uncertainty of the lower Sudakov limit (that gives a rough

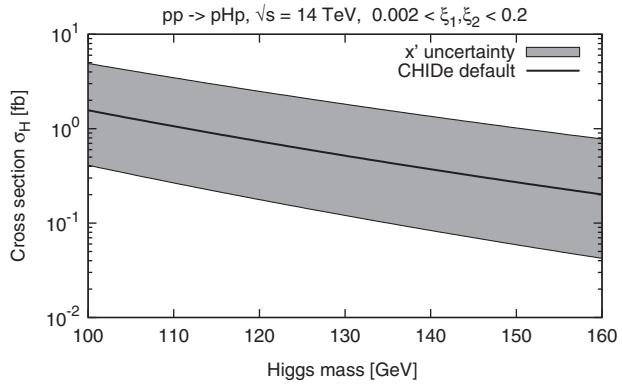

FIG. 14. Effect of varying the lower limit of the Sudakov form factor on the exclusive Higgs production at the LHC.

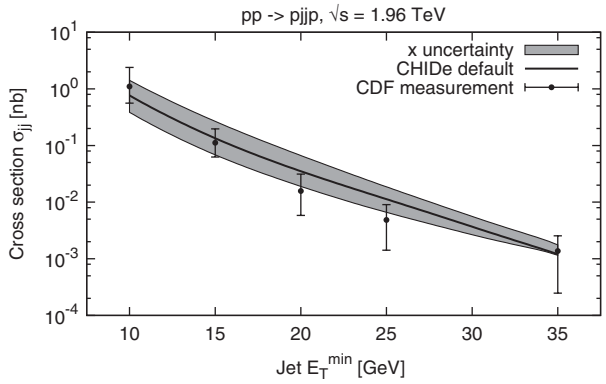

FIG. 15. Effect of varying the upper limit of Sudakov form factor on the exclusive jets production at the Tevatron.

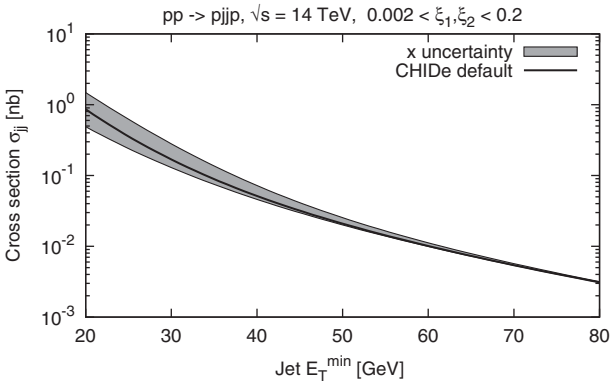

FIG. 16. Effect of varying the upper limit of the Sudakov form factor on the exclusive jets production at the LHC.

estimation of the uncertainty coming from the constant terms in the Sudakov form factor) for both jet and the Higgs boson production. Also, at the LHC the uncertainty of the upper limit can be neglected. However this does not lead to a good estimation of the total uncertainties on the Higgs cross section at the LHC. We need to check that the variation of those parameters are compatible with the CDF measurement. In the next section, we will study how to calculate the total uncertainty and how to reduce it—for the Higgs boson production—using a possible early measurement of exclusive jet at the LHC.

VI. PREDICTIONS FOR THE LHC

To make predictions for Higgs boson production at the LHC, we need to constrain the model parameters using the Tevatron data. The basic idea is to fit the model parameters to the CDF measurement and extrapolate the model to the center-of-mass energy of the LHC. We already know that the effect of the upper limit of integration in the Sudakov form factor will be negligible for high E_T jets at the LHC compared to the effects from the lower limit and the gluon density uncertainty. Varying the upper limit is not relevant for Higgs production as we already mentioned in the previous section.

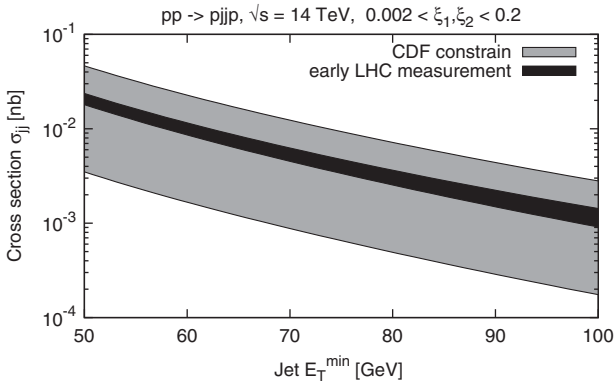

FIG. 17. Total uncertainty on the CHIDe model from the fit to the CDF measurement (light gray) and possible exclusive jets measurement with a low luminosity of 100 pb^{-1} at the LHC (dark gray).

To study the impact of the uncertainties on the Higgs and jet cross sections at the LHC, we need to take into consideration both the gluon uncertainty and the lower limit of the Sudakov form factor calculation. The principle is simple: for each gluon density (FIT1 to FIT4), we choose the x' values which are compatible with the CDF measurement to ensure that the model is indeed compatible with Tevatron data for this given gluon density. Taking into account the CDF data error, the procedure leads to two values of x', namely x'_{min} and x'_{max}, for each gluon density. The same x' values are used at LHC energies to predict the jet and Higgs boson cross sections—the total uncertainty range is taken as the extreme values predicted by all gluon densities, for appropriately x'_{min} or x'_{max}. The results are shown in Figs. 17 and 18. The obtained uncertainty is large, being greater than a factor of 10 for jets and about 25 for Higgs production.

To study how the uncertainties on exclusive Higgs boson production can be reduced, it is useful to check what the impact of the measurement of exclusive jets at the LHC will be. This is quite relevant in order to reduce the present

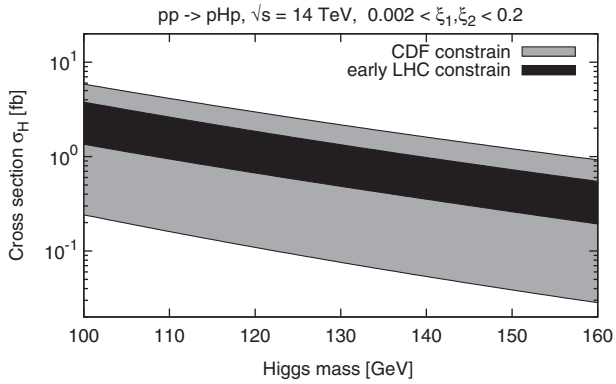

FIG. 18. Total uncertainty on the CHIDe model for exclusive Higgs production at the LHC: constraint from the fit to the CDF measurement (light gray), constraint from possible early LHC jets measurements with 100 pb^{-1} (dark gray).

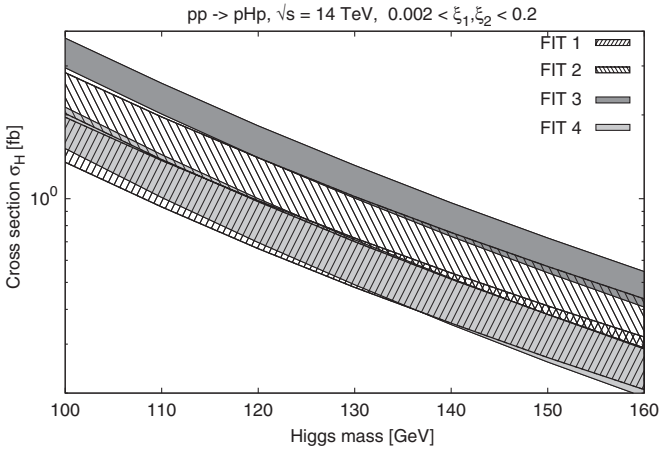

FIG. 19. Contributions to the total uncertainty on the CHIDe model for exclusive Higgs production at the LHC. For each gluon density (FIT1–FIT4) the x' uncertainty is shown for a luminosity of 100 pb^{-1}.

uncertainty on the Higgs boson cross section. We assume a possible early LHC measurement of exclusive jets cross section for 100 pb^{-1}. In addition to the statistical uncertainties, we consider a 3% jet energy scale uncertainty as the dominant contribution to the systematic uncertainty. This is quite conservative but takes into account other sources of uncertainties such as jet energy resolution and we assume this measurement to be performed at the beginning of the data taking of the LHC when all detectors are not yet fully understood. A possible result of such measurement is presented in Fig. 17. It is clearly visible that even very early LHC data can constrain the models much more than the Tevatron.

To check how this new measurement can constrain further the model uncertainties, we follow the same procedure as in the beginning of this section when we used the CDF data. For each gluon density, a range in x' describing the exclusive jets measurement at the LHC is chosen. The LHC early measurement can constrain the uncertainty on the Higgs boson production cross section to about a factor 5, as shown in Fig. 18. The exclusive jet cross section measurement at the LHC allows to constrain the x' parameter for each gluon distribution. Figure 19 shows the uncertainty of each gluon density separately. Although the uncertainty caused by the x' values is small, the remaining uncertainty due to the different gluon densities is large. Therefore some other measurements such as the exclusive photon production are needed to constrain further the Higgs cross section at the LHC.

VII. CONCLUSIONS

The KMR and CHIDe models of the exclusive jets and Higgs production have been implemented in the FPMC generator. They both show very similar, good description of exclusive jets measurement at the Tevatron energy. Although the predictions for the LHC energy show large differences, they are within the uncertainties of the models.

The main sources of uncertainties at LHC energies are the uncertainties on the gluon density in the soft region and the Sudakov form factor. Taking them into account, the results of the KMR and CHIDe models are compatible. The total uncertainty estimated from the CHIDe model predictions is quite large—a factor 10 for jets and 25 for Higgs, after taking into account the constraint coming from the CDF exclusive jets measurement. In addition, the uncertainty related to the variation of the limits in the Sudakov correction can be part of the uncertainty on the gluon unintegrated density and there is no obvious way to distinguish between them. This justifies the method of analysis we used in the previous section. Further measurements at the Tevatron (χ_c for which there is no Sudakov form factor or exclusive photons) will constrain the model further. We get the upper bound of the uncertainties that can be greatly reduced when measurements of the exclusive jets at the LHC are available. An early measurement using 100 pb^{-1} can constrain the Higgs production cross section by a factor of 5.

ACKNOWLEDGMENTS

A. D. would like to thank J.-R. Cudell and I. P. Ivanov for discussions and corrections as well as the CEA-Saclay for its support.

[1] V. A. Khoze, A. D. Martin, and M. G. Ryskin, Eur. Phys. J. C **19**, 477 (2001); **14**, 525 (2000); A. B. Kaidalov, V. A. Khoze, A. D. Martin, and M. G. Ryskin, Eur. Phys. J. C **21**, 521 (2001).

[2] M. Boonekamp, R. B. Peschanski, and C. Royon, Phys. Lett. B **598**, 243 (2004); M. Boonekamp, R. B. Peschanski, and C. Royon, Phys. Rev. Lett. **87**, 251806 (2001); M. Boonekamp, R. B. Peschanski, and C. Royon, Nucl. Phys. **B669**, 277 (2003); **B676**, 493(E) (2004).

[3] R. S. Pasechnik, A. Szczurek, and O. V. Teryaev, Phys. Rev. D **81**, 034024 (2010).

[4] R. S. Pasechnik, A. Szczurek, and O. V. Teryaev, Phys. Lett. B **680**, 62 (2009).

[5] J. R. Cudell, A. Dechambre, O. F. Hernandez, and I. P. Ivanov, Eur. Phys. J. C **61**, 369 (2009).

[6] M. G. Albrow and A. Rostovtsev, Report No. FERMILAB-PUB-00-173 (2000), p. 12.

[7] R. Staszewski and J. Chwastowski, Nucl. Instrum. Methods Phys. Res., Sect. A **609**, 136 (2009).

[8] A. Bialas and P. V. Landshoff, Phys. Lett. B **256**, 540 (1991).
[9] A. Schafer, O. Nachtmann, and R. Schopf, Phys. Lett. B **249**, 331 (1990).
[10] A. Bzdak, Acta Phys. Pol. B **35**, 1733 (2004).
[11] A. Bzdak, Phys. Lett. B **608**, 64 (2005).
[12] D. Kharzeev and E. Levin, Phys. Rev. D **63**, 073004 (2001).
[13] A. D. Martin and M. G. Ryskin, Phys. Rev. D **64**, 094017 (2001).
[14] J. R. Cudell and O. F. Hernandez, Nucl. Phys. **B471**, 471 (1996).
[15] I. P. Ivanov, N. N. Nikolaev, and A. A. Savin, Phys. Part. Nucl. **37**, 1 (2006).
[16] V. A. Khoze, A. D. Martin, and M. G. Ryskin, arXiv:hep-ph/0006005.
[17] T. D. Coughlin and J. R. Forshaw, J. High Energy Phys. 01 (2010) 121; T. D. Coughlin, Thesis: Central Exclusive Production.
[18] Y. L. Dokshitzer, D. Diakonov, and S. I. Troian, Phys. Rep. **58**, 269 (1980).
[19] L. Frankfurt, C. E. Hyde, M. Strikman, and C. Weiss, Phys. Rev. D **75**, 054009 (2007).
[20] L. A. Harland-Lang, V. A. Khoze, M. G. Ryskin, and W. J. Stirling, Eur. Phys. J. C **69**, 179 (2010).
[21] M. Gluck, E. Reya, and A. Vogt, Eur. Phys. J. C **5**, 461 (1998).
[22] A. D. Martin, R. G. Roberts, W. J. Stirling, and R. S. Thorne, Phys. Lett. B **443**, 301 (1998).
[23] H. L. Lai and W. K. Tung, Z. Phys. C **74**, 463 (1997).
[24] I. P. Ivanov and N. N. Nikolaev, Phys. Rev. D **65**, 054004 (2002).
[25] I. P. Ivanov, arXiv:hep-ph/0303053.
[26] V. A. Khoze, A. D. Martin, and M. G. Ryskin, Eur. Phys. J. C **18**, 167 (2000).
[27] A. Dechambre, Ph.D. thesis, University of Liege, 2010, http://hdl.handle.net/2268/7555.
[28] T. D. Coughlin and J. R. Forshaw (private communication).
[29] M. Boonekamp, V. Juranek, O. Kepka, and C. Royon, arXiv:0903.3861.
[30] G. Corcella, I. G. Knowles, G. Marchesini, S. Moretti, K. Odagiri, P. Richardson, M. H. Seymour, and B. R. Webber (HERWIG 6.5), J. High Energy Phys. 01 (2001) 010.
[31] V. A. Khoze, A. D. Martin, and M. G. Ryskin, Eur. Phys. J. C **23**, 311 (2002).
[32] J. Monk and A. Pilkington, Comput. Phys. Commun. **175**, 232 (2006).
[33] T. Aaltonen *et al.* (CDF Collaboration), Phys. Rev. D **77**, 052004 (2008).